REGULAR ARTICLE

blood advances

Distinct clinical characteristics of *DUX4*- and *PAX5*-altered childhood B-lymphoblastic leukemia

Zhenhua Li,[1] Shawn Hsien Ren Lee,[2] Winnie Hui Ni Chin,[1] Yi Lu,[1] Nan Jiang,[1] Evelyn Huizi Lim,[1] Elaine Coustan-Smith,[1] Kean Hui Chiew,[1] Bernice Ling Zhi Oh,[2] Grace Shimin Koh,[3] Zhiwei Chen,[1] Shirley Kow Yin Kham,[1] Thuan Chong Quah,[1,2] Hai Peng Lin,[4] Ah Moy Tan,[5] Hany Ariffin,[6] Jun J. Yang,[7] and Allen Eng-Juh Yeoh[1,2,8]

[1]Department of Paediatrics, VIVA-NUS Centre for Translational Research in Acute Leukaemia , Yong Loo Lin School of Medicine, National University of Singapore, Singapore; [2]Viva-University Children's Cancer Centre, Khoo Teck Puat-National University Children's Medical Institute, National University Hospital, National University Health System, Singapore; [3]Dean's Office, Yong Loo Lin School of Medicine, National University of Singapore, Singapore; [4]Subang Jaya Medical Centre, Subang Jaya, Malaysia; [5]Department of Paediatrics, Kandang Kerbau Women's and Children's Hospital, Singapore; [6]University of Malaya Cancer Research Institute, Faculty of Medicine, University of Malaya, Kuala Lumpur, Malaysia; [7]Department of Pharmaceutical Sciences, St. Jude Children's Research Hospital, Memphis, TN; and [8]Cancer Science Institute of Singapore, National University of Singapore, Singapore

Key Points

- Despite poor end-of-induction MRD, *DUX4* B-ALL has excellent outcome.
- *PAX5*alt B-ALL with IKZF1 codeletion is associated with poor outcome, which can be improved by treatment intensification.

Among the recently described subtypes in childhood B-lymphoblastic leukemia (B-ALL) were *DUX4*- and *PAX5*-altered (*PAX5*alt). By using whole transcriptome RNA sequencing in 377 children with B-ALL from the Malaysia-Singapore ALL 2003 (MS2003) and Malaysia-Singapore ALL 2010 (MS2010) studies, we found that, after hyperdiploid and *ETV6-RUNX1*, the third and fourth most common subtypes were *DUX4* (n = 51; 14%) and *PAX5*alt (n = 36; 10%). *DUX4* also formed the largest genetic subtype among patients with poor day-33 minimal residual disease (MRD; n = 12 of 44). But despite the poor MRD, outcome of *DUX4* B-ALL was excellent (5-year cumulative risk of relapse [CIR], 8.9%; 95% confidence interval [CI], 2.8%-19.5% and 5-year overall survival, 97.8%; 95% CI, 85.3%-99.7%). In MS2003, 21% of patients with *DUX4* B-ALL had poor peripheral blood response to prednisolone at day 8, higher than other subtypes (8%; $P = .03$). In MS2010, with vincristine at day 1, no day-8 poor peripheral blood response was observed in the *DUX4* subtype ($P = .03$). The *PAX5*alt group had an intermediate risk of relapse (5-year CIR, 18.1%) but when *IKZF1* was not deleted, outcome was excellent with no relapse among 23 patients. Compared with MS2003, outcome of *PAX5*alt B-ALL with *IKZF1* codeletion was improved by treatment intensification in MS2010 (5-year CIR, 80.0% vs 0%; $P = .05$). In conclusion, despite its poor initial response, *DUX4* B-ALL had a favorable overall outcome, and the prognosis of *PAX5*alt was strongly dependent on *IKZF1* codeletion.

Introduction

The most common type of cancer in children is B-cell lymphoblastic leukemia (B-ALL). B-ALL is biologically heterogeneous, driven by recurrent chromosomal aneuploidies, specific oncogene fusions, or more recently described point mutations.[1] These specific, recurrent genetic changes give rise to multiple genetic subtypes. Techniques based on next-generation sequencing have revealed the presence of >20 different subtypes of B-ALL, each with its own specific risk of relapse.

Submitted 1 April 2021; accepted 11 July 2021. prepublished online on *Blood Advances* First Edition 21 September 2021; final version published online 7 December 2021. DOI 10.1182/bloodadvances.2021004895.

Presented in part at the 61st American Society of Hematology Annual Meeting and Exposition, Orlando, FL, December 7-10, 2019.

For data sharing requests, contact the corresponding author (paeyej@nus.edu.sg).

The full-text version of this article contains a data supplement.

In 2002, we first described the unique gene expression signature of a novel group of B-ALLs.[2] It took 14 years to finally determine that this novel group is driven by the excessive expression of rearranged *DUX4*.[3-5] The challenge in elucidating the driver of *DUX4* B-ALL was its highly varied fusion junction and the relatively small size of the genome that is structurally affected. Its most common fusion is with the highly variable *IGH* gene, which could be deciphered only by using next-generation sequencing. *DUX4* drives leukemogenesis by dysregulating *ERG*, either directly or more commonly with deletion of the *ERG* gene.[5]

PAX5 is commonly deleted in many subtypes of B-ALL such as *ETV6-RUNX1*. In these subtypes, *PAX5* deletion is a cooperative mutation, not a driver mutation. However, 2 subtypes of B-ALL have distinct alterations in the *PAX5* gene as the driver: the *PAX5*-altered (*PAX5*alt) and the *PAX5* P80R point mutation subtypes.[6-8] Using gene expression profiling, *PAX5*alt and *PAX5* P80R are genetically distinct. The *PAX5*alt subtype commonly has codeletion of the *IKZF1* and *CDKN2A/B* genes, giving rise to the poorer outcome *IKZF1*^{plus} subtype.[9] *PAX5*alt and *PAX5* P80R are now considered as distinct genetic subtypes.

We used RNA-sequencing (RNA-seq) and multiplex-ligation–dependent probe amplification (MLPA) to analyze leukemic cells collected at diagnosis from 377 children with B-ALL treated on the Malaysia-Singapore ALL 2003 and 2010 studies (MS2003 and MS2010). We found that *DUX4* and *PAX5*alt subtypes, which formed the third and fourth largest genetic subtypes, had unique treatment responses that influenced the way they should be treated clinically.

Methods

Patients and materials

Bone marrow (BM) or peripheral blood (PB) samples at diagnosis (n = 387, including 7 patients treated off-protocol who were consented using cell bank consents) were collected from children (younger than age 18 years) with B-ALL enrolled in the MS2003 and MS2010 studies.[10,11] After subjecting the data to quality control, 377 patients qualified for analysis (Figure 1). The studies were approved by the National Healthcare Group (Singapore) domain-specific review board ref: 2004/00275, 2008/00081. Informed consent was obtained in accordance with the Declaration of Helsinki. At day 8 of remission induction, absolute blast count $\geq 1 \times 10^9$/L was defined as poor PB response. Minimal residual disease (MRD) was quantified using real-time quantitative polymerase chain reaction (RT-qPCR) with immunoglobulin and T-cell receptor PCR targets at a sensitivity of 1×10^{-4} and interpreted according to EuroMRD guidelines.[12] At the end of induction (EOI), which was at day 33, MRD $> 1 \times 10^{-4}$ was considered positive, and MRD $\geq 1 \times 10^{-2}$ was designated as MRD high risk (HR).

Conventional subtype classification

Conventional genetic subtyping was performed on diagnostic samples by using oncogene fusion panels, cytogenetics, and the DNA index. Rearrangements of *ETV6-RUNX1*, *BCR-ABL1*, *TCF3-PBX1*, *KMT2A-MLLT3*, *KMT2A-AFF1* (AF4), *KMT2A-MLLT1* (ENL), and *KMT2A-MLLT3* (AF9) were tested by using RT-qPCR oncogene fusion panels. Cytogenetics results for samples with >50 modal chromosomes (or DNA index ≥1.16) were classified as high hyperdiploid and samples with <44 modal chromosomes were classified as hypodiploid. *BCR-ABL1*, *KMT2A*-rearranged, and hypodiploid ALL were classified as HR subtypes, and *ETV6-RUNX1* and high hyperdiploid were classified as low-risk (LR) subtypes.

RNA-seq and data analysis

RNA-seq was performed on bulk diagnostic samples (without cell sorting) using TruSeq stranded messenger RNA (mRNA) library prep kit (Illumina, San Diego, CA), and the samples were sequenced using the Illumina HiSeq 2000/2500 platform with a read length of 2×101 or a NextSeq 500 platform with a read length of 2×151. Reads were mapped to the hg19 reference genome using Tophat2.[13] To minimize the difference between the 2 platforms due to the read length, reads from the NextSeq 500 platform were trimmed to the same read length as HiSeq reads before alignment. Samples with low coverage (10× exonic region coverage ≤30%) or strong 5' to 3' bias (≤0.3 or ≥3) were removed (Figure 1).

The number of reads mapped to each gene were counted by using featureCounts.[14] Gene expression levels were normalized by using variance stabilizing transformation from the DESeq2 package[15] followed by batch effect correction using the sva package.[16] To select the genes for hierarchical clustering, we first selected genes with significantly higher variance in B-ALL compared with T-cell ALL (T-ALL; n = 37) by nonparametric Conover squared ranks test[17] with adjusted *P* value (by Holm's method[18]) < .05. This helped exclude the genes with high but irrelevant variance (eg, variance as a result of sex, race, or circadian rhythm). The top 500 in the remaining gene set with the highest median absolute deviation were used in the hierarchical clustering, with Ward's algorithm[19] and correlation coefficient as the distance metric.

Gene rearrangements were detected using FusionCatcher.[20] Variant calling based on RNA-seq data was carried out according to the GenomeAnalysisToolkit (GATK) best practices for variant calling[21] and annotated with the Variant Effect Predictor.[22] Briefly, reads were aligned to the hg19 reference by using 2-pass alignment by Spliced Transcripts Alignment to a Reference (STAR).[23] Aligned reads were subjected to sorting by coordinate, duplicate removal, split at the splicing sites, and variant calling by HaplotypeCaller. Variations with significant strand bias (Phred-scaled *P* value >30), depth normalized quality score <2.0, or clustered with 3 or more in a window of 35 bases were removed. Digital karyotyping (or gross copy number variation [CNV] identification) for autosomes and chromosome X were performed using the method described by Gu et al.[7]

CNVs by multiplex ligation-dependent probe amplification

CNVs in *IKZF1*, *PAX5*, *CDKN2A*, *CDKN2B*, *ERG*, and *ETV6* genes were screened using MLPA assay with SALSA probe mixes P335 and P327 (MRC-Holland, Amsterdam, The Netherlands) according to the manufacturer's protocol. MLPA output was analyzed using Coffalyser.Net (MRC-Holland) with the default program setting and recommended cutoff values of ≤0.7 for deletion and ≥1.3 for duplication.

Statistical analysis

All statistical analyses were performed using Windows R version 3.5.2. Cumulative risk of relapse (CIR) was compared by using Gray's test,[24] and overall survival (OS) was compared by using a log-rank test.[25] Competing risk regression[26] and Cox regression[27] were used for multivariable analysis for CIR and OS, respectively.

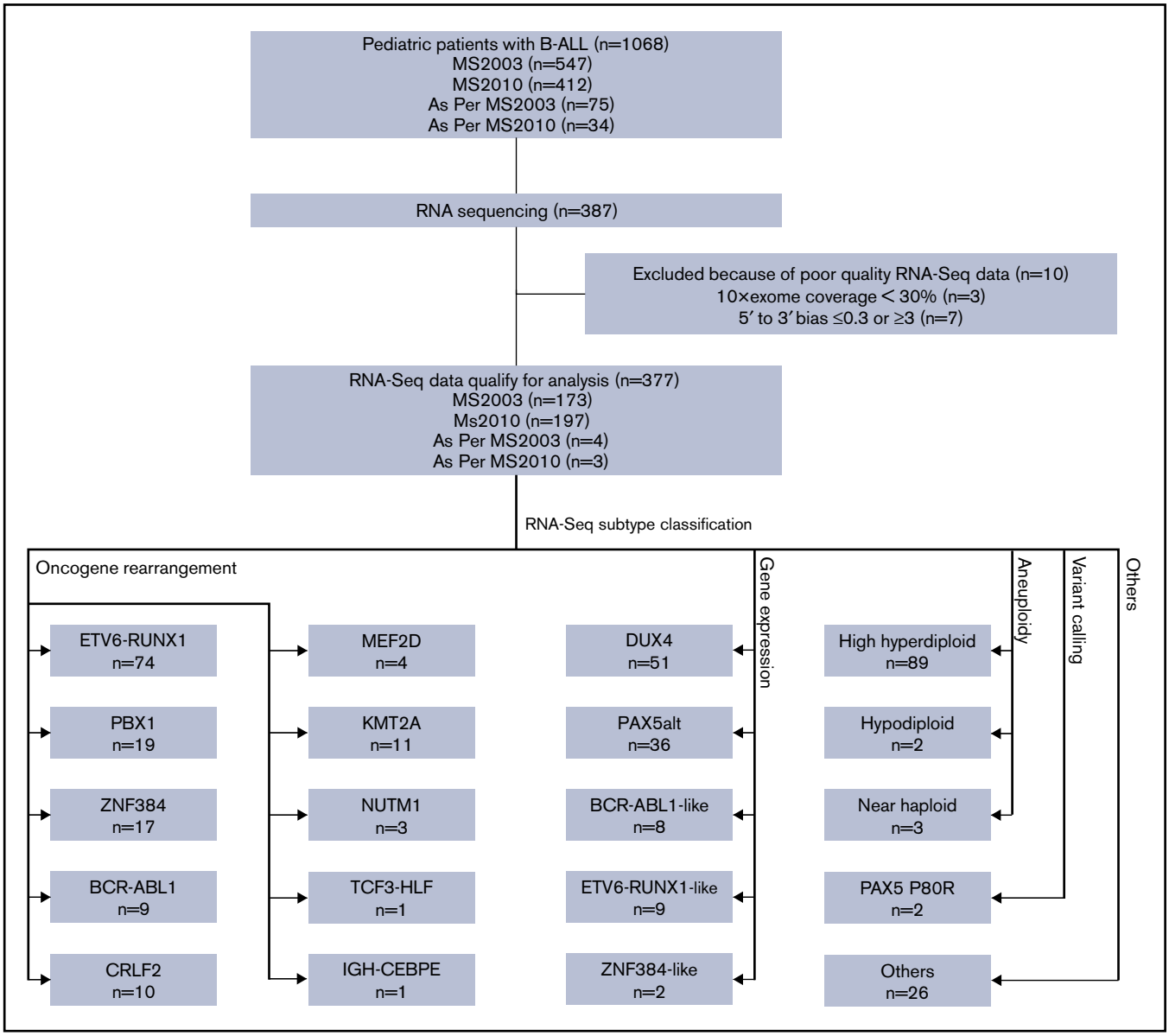

Figure 1. Diagram of RNA-seq and subtype classification of patients with B-ALL. RNA-seq was performed on a subset of patients with B-ALL enrolled in the MS2003 and MS2010 studies (including a few treated as per protocol). After quality control, RNA-seq data of 377 patients qualified for analysis. Patients were classified into 20 subtypes using 4 different methods. Some subtypes may be classified with multiple methods; only the leading method is indicated (Table 1).

Time-to-event was recorded from the diagnosis to relapse or death. When no event was observed, the patient was censored at the date of last contact. Resistant disease (BM blasts >5% at day 33) was considered as an event at day 1. Independence of categorical variables was tested using a χ^2 test. All tests were two-sided, unless otherwise specified.

Results

Classification of B-ALL using a single platform (RNA-seq)

By using RNA-seq, we performed digital karyotyping, identification of oncogene rearrangements, gene expression unsupervised hierarchical clustering, and variant calling. We were able to classify patients into 20 genetic subtypes with specific genomic alterations (Figure 1; Table 1). The subtypes showed distinct gene expression profiles by hierarchical clustering (Figure 2).

Distinct gene expression signatures defined 5 subtypes (Table 1): *DUX4*, *PAX5*alt, *ETV6-RUNX1*-like, *BCR-ABL1*-like, and *ZNF384*-like. Because the *DUX4-IGH* rearrangement could not be reliably identified, we defined the *DUX4* (14%; n = 51) subtype as the branch containing all identified *DUX4-IGH* rearrangements (n = 39). After high hyperdiploid and *ETV6-RUNX1*, *DUX4* subtype was the third most common subtype. All the patients in this branch (Figure 2) exclusively showed highly elevated expression of *DUX4* with >30 reads per million mapped reads.

Table 1. Definition and risk stratification of B-ALL subgroups using RNA-seq

Subtype	No. (N = 377)	%	Method	Criteria	5-y CIR (%)	95% CI	5-y OS (%)	95% CI	RNA-seq risk stratification
High hyperdiploid	89	24	a	No. of chromosomes >50	5.5	1.7-12.6	98.8	91.8-99.8	Low
Hypodiploid	2	1	a	No. of chromosomes 31-44	50.0	0.0-96.0	50.0	0.6-91.0	High
Near haploid	3	1	a	No. of chromosomes 24-30	50.0	0.0-96.0	50.0	0.6-91.0	High
ETV6-RUNX1	74	20	b	*ETV6-RUNX1* rearrangement	5.2	1.3-13.1	100.0	100.0	Low
ETV6-RUNX1-like	9	2	c	Coclustered with *ETV6-RUNX1* rearrangement	12.7	0.5-45.3	88.9	43.3-98.4	Intermediate
DUX4	51	14	c	In the cluster containing all *DUX4-IGH* rearrangements	8.9	2.8-19.5	97.8	85.3-99.7	Low
PBX1	19	5	b	*PBX1* rearrangement	5.6	0.3-23.1	94.4	66.6-99.2	Intermediate
ZNF384	17	5	b	*ZNF384* rearrangement	6.3	0.4-25.5	93.3	61.3-99.0	Low (EP300) Intermediate (other partners)
ZNF384-like	2	1	c	Coclustered with *ZNF384* rearrangement	NA		NA		Intermediate
BCR-ABL1	9	2	b	*BCR-ABL1* rearrangement	37.5	7.2-69.4	75.0	31.5-93.1	High
BCR-ABL1-like	8	2	c+b	Coclustered with *BCR-ABL1*, no *CRLF2* rearrangement	37.5	6.9-69.8	75.0	31.5-93.1	High
CRLF2	10	3	b	*CRLF2* rearrangement	20.0	2.6-49.2	59.1	16.0-86.0	High
MEF2D	4	1	b	*MEF2D* rearrangement	0.0	0.0	100.0	100.0	High
KMT2A	11	3	b	*KMT2A* rearrangement	54.3	16.7-81.2	64.8	25.3-87.2	High
NUTM1	3	1	b	*NUTM1* rearrangement	0.0	0.0	100.0	100.0	Intermediate
*PAX5*alt	36	10	c+a+b+d	In the cluster enriched with *PAX5* alterations; no other subtype-defining events	18.1	6.3-34.7	89.2	69.7-96.5	Intermediate
PAX5 P80R	2	1	d+c	*PAX5* P80R mutation, clustered separately	NA		NA		Intermediate
TCF3-HLF	1	0.3	b	*TCF3-HLF* rearrangement	NA		NA		High
IGH-CEBPE	1	0.3	b	*IGH-CEBPE* rearrangement	0.0	0.0	100.0	100.0	Intermediate
Others	26	7	a+b+c+d	Other patients	20.7	7.3-39.0	94.1	65.0-99.1	Intermediate

The methods used to define each subgroup can be categorized into 4 types: (a) digital karyotyping, (b) identification of oncogene rearrangement, (c) gene expression profiling, and (d) variant calling. Patients whose disease had multiple features were classified according to gene expression clustering.

The branch enriched in *PAX5* rearrangements[7] by hierarchical clustering defined the *PAX5alt* subtype (10%; n = 36). *PAX5*alt was the fourth most common subtype. One patient with *EPOR-IGH* rearrangements (and hemizygous *PAX5* deletion) clustered with *PAX5*-alt and not with *BCR-ABL1*, and was classified as *PAX5*alt. Another 5 patients (3 *CRLF2*, 1 *BCR-ABL1*, and 1 near-haploid subtype) clustered in this *PAX5*alt branch as well; 4 were positive for deletions or internal tandem duplication (ITD) of *PAX5* and 1 had no *PAX5* CNV data. These patients were classified by their driver mutations (ie, *CRLF2*, *BCR-ABL1*, and near haploid).

There were 3 subtypes that showed gene expression signatures similar to those of known subtypes (Table 1). Clustered with *ETV6-RUNX1* was the *ETV6-RUNX1*-like subtype (2%; n = 9). Of the 9 *ETV6-RUNX1*-like subtypes, 3 harbored *ETV6* rearrangements with alternative partners (*GIP*, *MKL1*, and *BCL2L14*) and 1 had *PHAX-IGH* rearrangement. All the patients with *ETV6-RUNX1*-like (with available data, n = 8 of 8; supplemental Figure 1) had *ETV6* deletion and most (n = 7 of 9; Figure 2) clustered within 1 sub-branch, indicating the uniqueness of the gene expression of this subtype. Notably, in 2 patients with *ETV6-RUNX1*-like subtypes, *ETV6* mutations (p.Trp360Arg and p.Glu364Ter) were identified by RNA-seq, both of which were previously reported to be damaging.[28] After excluding *CRLF2* rearrangements, the *BCR-ABL1*-like subtype (2%; n = 8) coclustered with *BCR-ABL1*, with 75% (6 of 8) having tyrosine kinase rearrangements, including *EBF1-PDGFRB* (n = 3), *ETV6-PDGFRB* (n = 1), *SSBP2-CSF1R* (n = 1), and *NUP214-ABL1* (n = 1). Two patients (1%) with gene expression signatures similar to those of patients with *ZNF384*-rearranged were classified as *ZNF384*-like. Two patients (1%) with unique gene expression signatures and *PAX5* P80R mutation were defined as *PAX5* P80R subtype. The high mutant allele frequencies of the *PAX5* P80R mutations (99.7% and 73.4%) suggested biallelic variations of *PAX5*, in agreement with previous studies.[6,7] The remaining patients were classified as B-Others (7%; n = 26).

Clinical characteristics of the subtypes

The RNA-seq genetic subtypes were strongly correlated with age at presentation ($P = 1.2 \times 10^{-37}$; Figure 2; supplemental Figure 2). The majority of patients with high hyperdiploid and *ETV6-RUNX1* subtypes were between age 1 and 10 years, whereas *DUX4*, *PAX5*alt, and *BCR-ABL1* (along with *BCR-ABL1*-like and *CRLF2*) subtypes were more common in patients older than age 10 years.

*PAX5*alt, *PBX1*, *BCR-ABL1*, *BCR-ABL1*-like, *CRLF2*, and *ETV6-RUNX1*-like subtypes were associated with high-presenting white blood cell count (WBC) $>50 \times 10^9$/L ($P = 6.5 \times 10^{-8}$; Figure 2; supplemental Figure 3). The genetic subtypes were marginally correlated with race ($P = .03$; supplemental Figure 4), and no significant correlation with sex or central nervous system (CNS) status was observed (supplemental Figure 5). The subtypes had different frequencies of *IKZF1* deletion (*IKZF1*^{del}; Figure 2). *IKZF1*^{del} was most frequent in *CRLF2* (80%), *ETV6-RUNX1*-like (63%), *BCR-ABL1*-like (60%), and *BCR-ABL1* (44%) subtypes but virtually absent in *PBX1*, *KMT2A*, and B-Others subtypes.

Interestingly, in unsupervised hierarchical clustering, *ETV6-RUNX1* had 2 sub-branches with distinctly different *PAX5* CNVs (Figure 2; supplemental Figure 6A). All but 1 of the samples with *PAX5* deletion were clustered in 1 sub-branch (Figure 2) with distinct gene expression signatures (supplemental Figure 6B). The *ETV6-RUNX1* subtype with *PAX5* deletions had significantly higher presenting WBC ($P = 4.8 \times 10^{-4}$; Figure 2; supplemental Figure 6A) but still had excellent outcome (CIR, 0%; supplemental Figure 6C).

DUX4 subtype had poorer EOI MRD but good outcome

The largest subtype in the EOI MRD HR group was *DUX4*. *DUX4* accounted for 27% (n = 12 of 44; supplemental Figure 7) of the MRD HR patients. Conversely, 24% of the patients (12 of 50) with the *DUX4* subtype were EOI MRD HR, significantly higher than 11% in other subtypes ($P = 8.2 \times 10^{-3}$; Figure 3A). Only 22% of the patients with *DUX4* subtype were EOI MRD negative ($\leq 1 \times 10^{-4}$), significantly less than 52% in other subtypes ($P = 7.7 \times 10^{-5}$; Figure 3A). Interestingly, most of the patients with *DUX4* subtype with negative day-33 EOI MRD had ERG codeletion (details are provided in the following section).

MS2003 induction[10] consisted of the standard ALL Berlin-Frankfurt-Münster (BFM) single dose of intrathecal methotrexate (IT MTX) at day 1 followed by 7 days of prednisolone (PRED). In the MS2010 protocol,[11] the day 1 IT MTX was replaced with intravenous vincristine (IV VCR). We compared the day-8 PB response in the MS2003 and MS2010 studies to investigate the initial response of patients with the *DUX4* subtype. In MS2003, patients with the *DUX4* subtype had significantly higher frequency of day-8 PB poor response than other subtypes (21% vs 8%; $P = .03$; Figure 3B), suggesting that the *DUX4* subtype was relatively resistant to PRED. In MS2010, the *DUX4* subtype had no poor day-8 PB responders ($P = .03$; Figure 3B), suggesting that IV VCR was more effective.

Despite the poorer EOI MRD, the outcome for patients with the *DUX4* subtype was excellent: the 5-year CIR was 8.9% (95% confidence interval [CI], 2.8%-19.5%), and the 5-year OS was 97.8% (95% CI, 85.3%-99.7%). This excellent outcome was comparable to other low-risk subtypes, including *ETV6-RUNX1* and high hyperdiploid (CIR, $P = .39$; OS, $P = .41$; Figure 3C-D) and was significantly better than that for high-risk subtypes of *BCR-ABL1*, *KMT2A*, hypodiploid, and near haploid (CIR, $P = 2.9 \times 10^{-4}$; OS, $P = 2.3 \times 10^{-4}$; Figure 3C-D). Interestingly, EOI and week 12 end-of-consolidation PCR MRD were not predictive of outcome in patients with the *DUX4* subtype (supplemental Figure 8). All 3 patients with *DUX4* who relapsed had negative week-12 MRD (supplemental Figure 8B); 2 of them retained the same PCR MRD clone, and another had isolated CNS relapse. Details for the patients with *DUX4* subtype are summarized in supplemental Table 1.

ERG deletion defined a subentity in *DUX4* B-ALL with better day-33 EOI MRD

A frequent secondary event in patients with the *DUX4* subtype[5,29] was *ERG* deletion. We performed MLPA for *ERG* CNV identification in 194 of the 377 patients, including 43 of the 51 with the *DUX4* subtype. Of the 25 patients with *ERG* deletion, 92% (n = 23) had the *DUX4* subtype, except for 1 *PAX5*alt and 1 *ZNF384*-like (Figure 3E). Within the *DUX4* subtype, *ERG* deletion was associated with better EOI MRD: 39% of patients were MRD negative compared with 5% of those with normal *ERG* ($P = 8.2 \times 10^{-3}$; Figure 3F). Consistent with previous findings,[5,30] *IKZF1*^{del} was not associated with increased risk of relapse in patients with the *DUX4* subtype with or without *ERG* deletion (supplemental Figure 9). Unsupervised hierarchical clustering showed that the *DUX4* subtype with *ERG* deletion had distinct gene expression profiles (Figure 3G), suggesting a subentity.

IKZF1 deletion was highly predictive of relapse in the *PAX5*alt subtype

PAX5 fusions occurred in 42% (15 of 36) of the patients with *PAX5*alt. The *PAX5* fusions had 11 different partners: *NOL4L* (n = 3) and *CBFA2T3* (n = 3) were the most common, followed by 9 fusions to *AUST2*, *CBFA2T2*, *ELN*, *ESRRA*, *FBRS*, *FBRSL1*, *FKBP15*, *PEG10*, and *ZCCHC7*, each occurring only once. *PAX5* deletions and ITDs occurred in 69% (22 of 32) of the patients with *PAX5*alt compared with 17% (50 of 289; $P = 3.6 \times 10^{-11}$; Figure 2) in other subtypes. In patients with the *PAX5*alt subtype who had CNV data, 84% (26 of 31) had *CDKN2A/B* deletions, significantly higher than the 23% (65 of 288; $P = 6.9 \times 10^{-13}$; Figure 2) in other subtypes.

In patients with the *PAX5*alt subtype, *IKZF1*^{del} was associated with a higher risk of relapse (CIR, 50.0% vs 0%; $P = 2.0 \times 10^{-3}$; Figure 4A; supplemental Table 2) as well as a trend toward poorer OS (Figure 4B). In the MS2010 trial, in which the treatment of all patients with *IKZF1*^{del} was intensified, *PAX5*alt with *IKZF1*^{del} had a lower relapse rate (CIR, 80% vs 0%; $P = .05$; Figure 4C) and a trend toward better OS (Figure 4D).

RNA-seq–defined genetic subtype improved risk stratification of B-ALL

We investigated risk stratification using RNA-seq–defined subtypes. Conventionally, high hyperdiploid and *ETV6-RUNX1* were considered LR, whereas *BCR-ABL1*, *KMT2A*, and hypodiploid (including near haploid) were considered HR. We reviewed the published survival outcomes of the recently discovered subtypes (supplemental Table 3) and assigned them to risk groups: *DUX4* to LR[7,8,29,31] and *BCR-ABL1*-like,[31,32] *CRLF2*,[31,33,34] *MEF2D*,[8,35-38] and *TCF3-HLF*[39-41] to HR. For the *ZNF384* subtype, we assigned patients with *ZNF384-EP300* to LR and patients with other *ZNF384* rearrangements to intermediate risk (IR), based on the results from the Ponte Di Legno Childhood ALL Working Group.[42] The remaining subtypes, including *PBX1*, *NUTM1*, *PAX5*alt, *PAX5* P80R, *IGH-CEBPE*, *ETV6-RUNX1*-like, *ZNF384*-like, and B-Others were classified as IR. Table 1 summarizes the MS2003 and MS2010 5-year

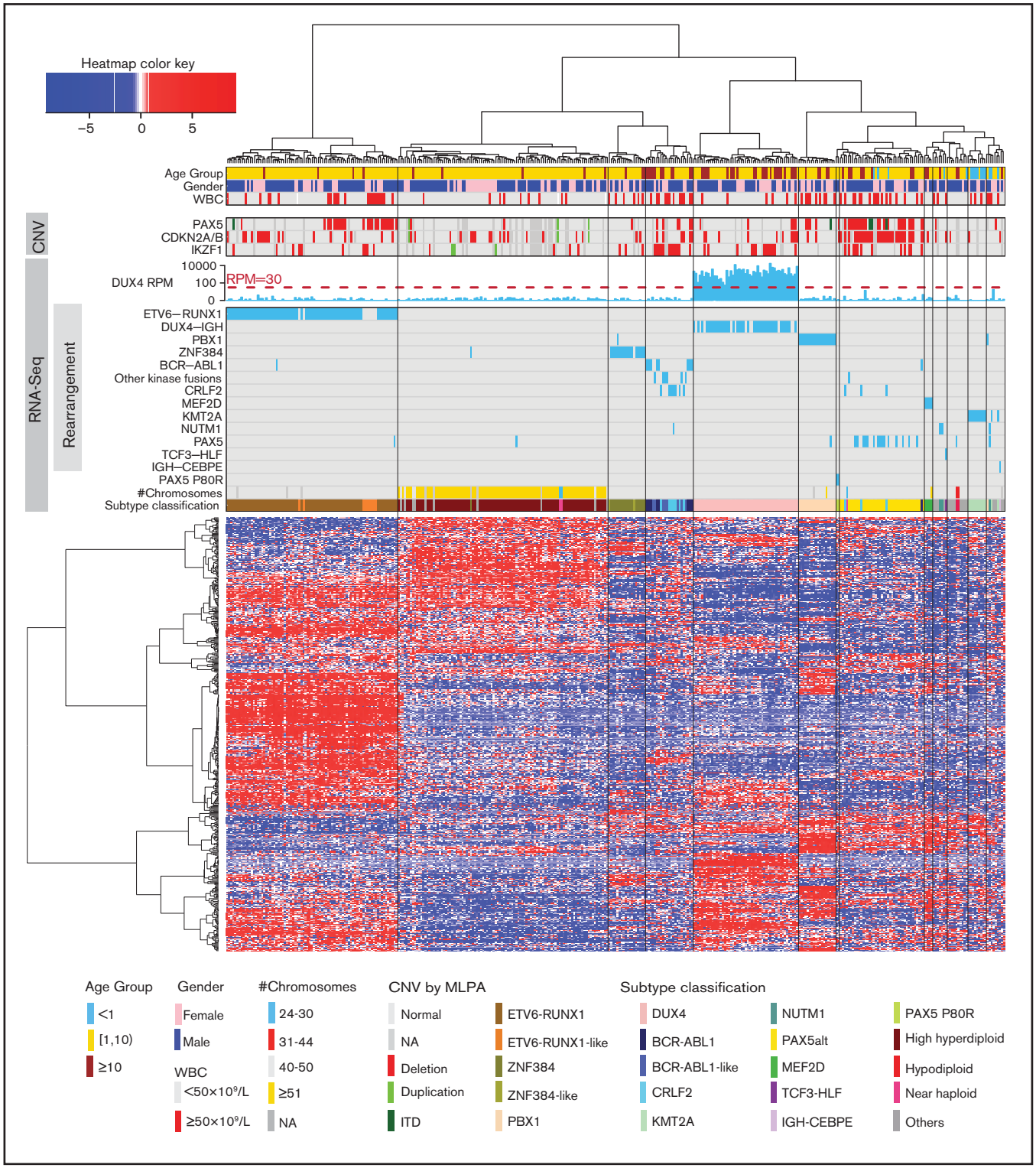

Figure 2. Unsupervised hierarchical clustering based on gene expression profiles. Hierarchical clustering, oncogene rearrangement identification, *PAX5* P80R variant calling, gross chromosome CNV detection, and subtype classification were performed using RNA-seq data. Age, sex, presenting WBC, and CNV of *PAX5*, *CDKN2A/B*, and *IKZF1* (by MLPA) are shown. These are not used in subtype classification. ITD, internal tandem duplication; NA, not available.

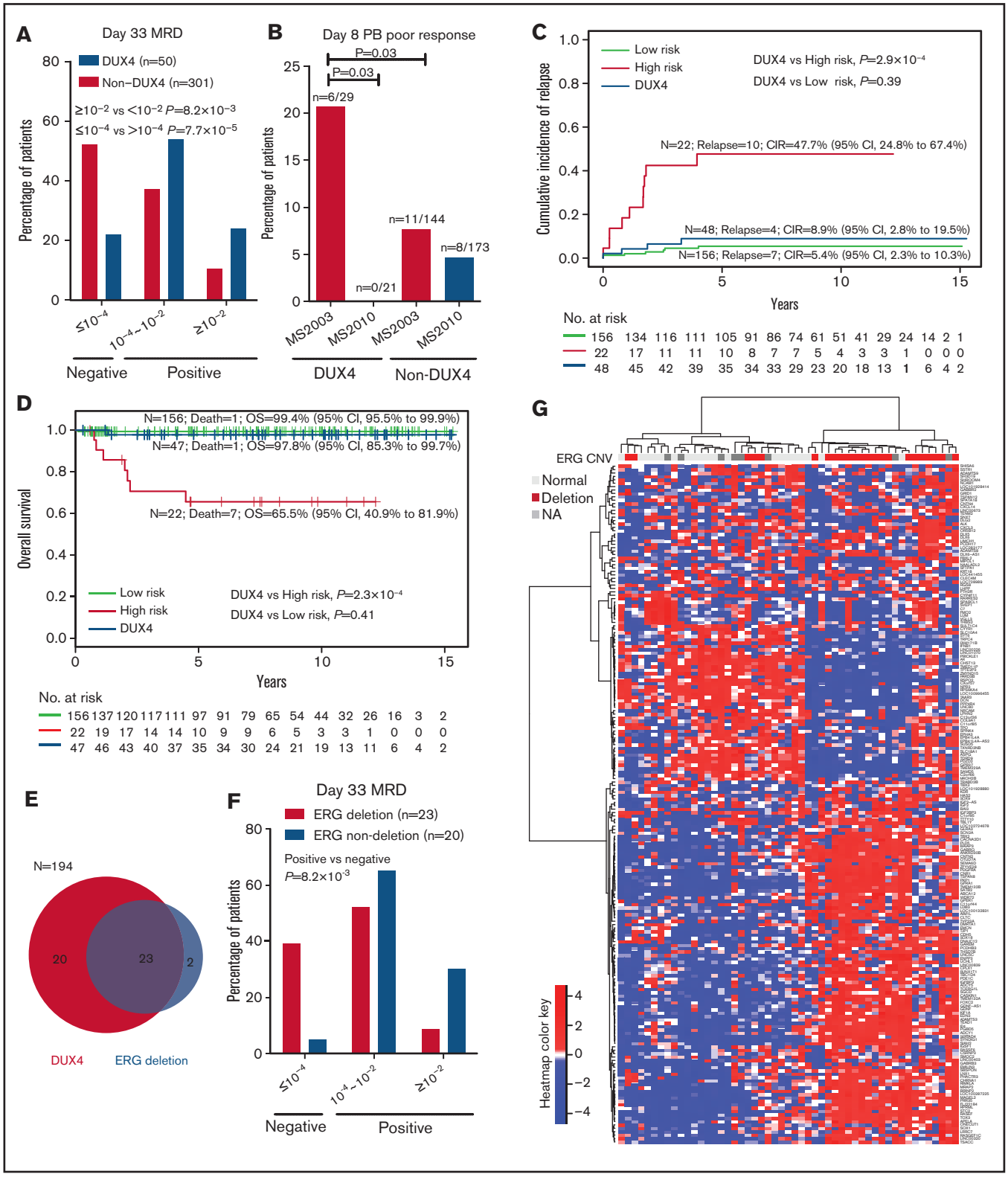

Figure 3. Distinct clinical characteristics of the *DUX4* subtype. (A) Patients with the *DUX4* subtype have higher day-33 MRD. (B) In MS2003, patients with the *DUX4* subtype had significantly poorer day-8 PB response than patients in MS2010, which used IV vincristine. CIR (C) and OS (D) of *DUX4* subtype compared with conventional LR subtypes (including *ETV6-RUNX1* and high hyperdiploid) and HR subtypes (including *BCR-ABL1*, *KMT2A*, hypodiploid, and near haploid). (E) Relationship between *ERG* deletion and *DUX4* subtype. (F) Patients with the *ERG* deletion in the *DUX4* subtype had better day-33 MRD. (G) Unsupervised hierarchical clustering of the *DUX4* subtype showing that ERG deletions are associated with distinct gene expression signatures. Genes with significantly higher variance in *DUX4* subtypes than the rest of the

CIR and 5-year OS by RNA-seq subtypes, which generally concurred with the published outcomes.

We then compared the survival outcomes of conventional risk stratification based on oncogene fusion, cytogenetics, and DNA index against RNA-seq subtype risk stratification (Table 1, last column). Although conventional laboratory test subtype assignment (Figure 5A-B) assigned only 5% (n = 17 of 362) patients into the HR group, 30% (n = 108) into LR group, and 65% (n = 237) into the large IR group, it was highly predictive of outcome (CIR, $P = 2.1 \times 10^{-7}$; OS, $P = 4.1 \times 10^{-7}$; event-free survival [EFS], $P = 8.9 \times 10^{-8}$; Figure 5; supplemental Figure 10). When subtype assignment was performed for all of the patients treated on MS2003 and MS2010, the CIR and OS of the risk groups were similar (supplemental Figure 11). If we used RNA-seq as a single platform to generate conventional subtype assignment (supplemental Figure 12), slightly more patients were assigned to HR (6%; n = 22) and LR (43%; n = 156) with similar outcome prediction (CIR, $P = 2.1 \times 10^{-7}$; OS, $P = 6.6 \times 10^{-8}$).

By incorporating the newly discovered genetic subtypes that could not be defined by conventional laboratory tests (Figure 5C-D), 57% (136 of 237) of the conventional IR patients were stratified to either LR (46.0%) or HR (11.4%; supplemental Figure 13). Specifically, RNA-seq assigned twofold more patients to the LR group (212 vs 108; Figure 5C compared with Figure 5A), with comparable CIR (6.0% vs 5.0%), EFS (93.5% vs 95%; supplemental Figure 10), and OS (99.0% vs 100%). The number of HR patients also increased more than twofold (45 vs 17), with lower CIR (37.4% vs 52.9%), higher EFS (55.7% vs 47.1%; supplemental Figure 10), yet similar OS (68.6% vs 64.7%). By conventional methods, most of the relapses and deaths were in the large IR group, which could not be stratified (69% relapses and 74% deaths). Using RNA-seq, the HR group had the most relapses (38%) and deaths (57%).

In a multivariable analysis model of competing risk regression on CIR controlling for age, sex, WBC, day-33 MRD, and treatment protocol (Table 2), RNA-seq risk stratification (IR vs LR: $P = .01$; HR vs LR: $P = 7.2 \times 10^{-4}$), EOI MRD (HR vs SR: $P = 2.0 \times 10^{-6}$), and treatment protocol (MS2010 vs MS2003: $P = .03$) remained significant.

In a Cox proportional hazards regression on OS with the same variables, only RNA-seq risk stratification (IR vs LR: $P = .02$; HR vs LR: $P = 1.6 \times 10^{-3}$) and age (≥10 vs 1-10 years: $P = .04$) were independently associated with OS; EOI MRD lost its significance. In each MRD risk group, RNA-seq risk stratification helped further refine prediction of OS (supplemental Figure 14). However, in each RNA-seq risk group, EOI MRD no longer predicted OS (supplemental Figure 15). When the treatment arms[10,11] were included in the multivariable analysis models, similar results were obtained (supplemental Table 4).

Discussion

We found that in B-ALL, the third and fourth most common subtypes were the recently described B-ALL subtypes–*DUX4* and *PAX5*alt; 14% of our study cohort had the *DUX4* subtype. Although patients with *DUX4* had significantly poorer EOI MRD response (78% EOI MRD positive compared with 48% in other subtypes; $P = 7.7 \times 10^{-5}$), they had an excellent outcome (5-year CIR, 8.9%; 5-year OS, 97.8%; Figure 3). We also found that although *PAX5*alt had intermediate outcome, that outcome was significantly influenced by codeletion of *IKZF1* (Figure 4). All 23 patients with *PAX5*alt with no deletion of *IKZF1* gene remained in continuous complete remission. Intensifying therapy in patients with *PAX5*alt with codeletion of *IKZF1* significantly reduced the risk of relapse ($P = .05$).

We confirmed that the *DUX4* subtype was more common among older children (median age at diagnosis, 9.8 years; supplemental Figure 2). But despite this National Cancer Institute HR age group, patients with *DUX4* had excellent outcomes (Figure 3C-D), similar to outcomes in other reports in both pediatric and adult patients.[7,8] However, 78% of patients with the *DUX4* subtype were EOI MRD positive, with 24% being EOI MRD HR (Figure 3A). In fact, the largest group of EOI MRD HR patients had the *DUX4* subtype (27%; n = 12 of 44). In MS2003, in which patients received only 1 dose of IT MTX and 7 days of oral PRED, patients with *DUX4* had a significantly poorer PB response ($P = .03$; Figure 3B). Adding VCR to the first 8 days of PRED in the MS2010 trial significantly improved PB response (Figure 3B).

Czech investigators reported[43] that during induction, *DUX4* blasts underwent a monocytic switch, which resulted in discrepant PCR-based and flow-based MRD. These monocytic switched blasts carried the PCR-based MRD markers but lost their flow-based CD19 markers. Because of this, flow-based MRD reported good MRD clearance, but PCR-based MRD showed a persistent high level of disease. In our own experience, in 4 patients with *DUX4* who had positive PCR MRD, flow MRD on the same sample was clearly negative (MRD <0.01%; unpublished data). Intriguingly, these monocytic blasts may not contribute to relapse. This might explain why despite having high EOI MRD, PCR-based MRD was not predictive of outcome in patients with *DUX4*. In patients with *DUX4*, flow-based MRD might be a better platform for risk stratification.

Most patients with *DUX4* B-ALL in MS2003 and MS2010 were treated in the HR or IR arm (88%; n = 45 of 51; supplemental Table 1) because of positive EOI MRD, older age, and frequent *IKZF1*^{del}. Yet the outcomes of patients with *DUX4* were excellent (5-year CIR, 8.9%; 5-year OS, 97.8%), which was similar to that for the favorable subtypes (5-year CIR in *ETV6-RUNX1*, 5.2%; high hyperdiploid, 5.5%; Table 1). This created a conundrum: was the good outcome of patients with the *DUX4* subtype a result of intensified therapy? Or, alternatively, was *DUX4* a favorable subtype?

To solve this conundrum, Jeha et al[44] recently reported on St. Jude's Total Therapy Study XVI for Newly Diagnosed Patients With Acute Lymphoblastic Leukemia (hereafter Total Therapy Study XVI), which had novel subtypes, including *DUX4*. None of their patients with *DUX4* (n = 20) were HR, 40% were LR, 60% were standard risk, and none received BM transplantation. Their 5-year EFS and OS were 95%, which was similar to our results. St. Jude's report

Figure 3. (continued) cohort (by Conover squared ranks test) with adjusted *P* value (by Holm's method) <.05 were first selected. In the selected genes, the top 200 genes with the highest median absolute deviation in *DUX4* subtype were used in hierarchical clustering using correlation coefficient as the distance metric and Ward's algorithm.

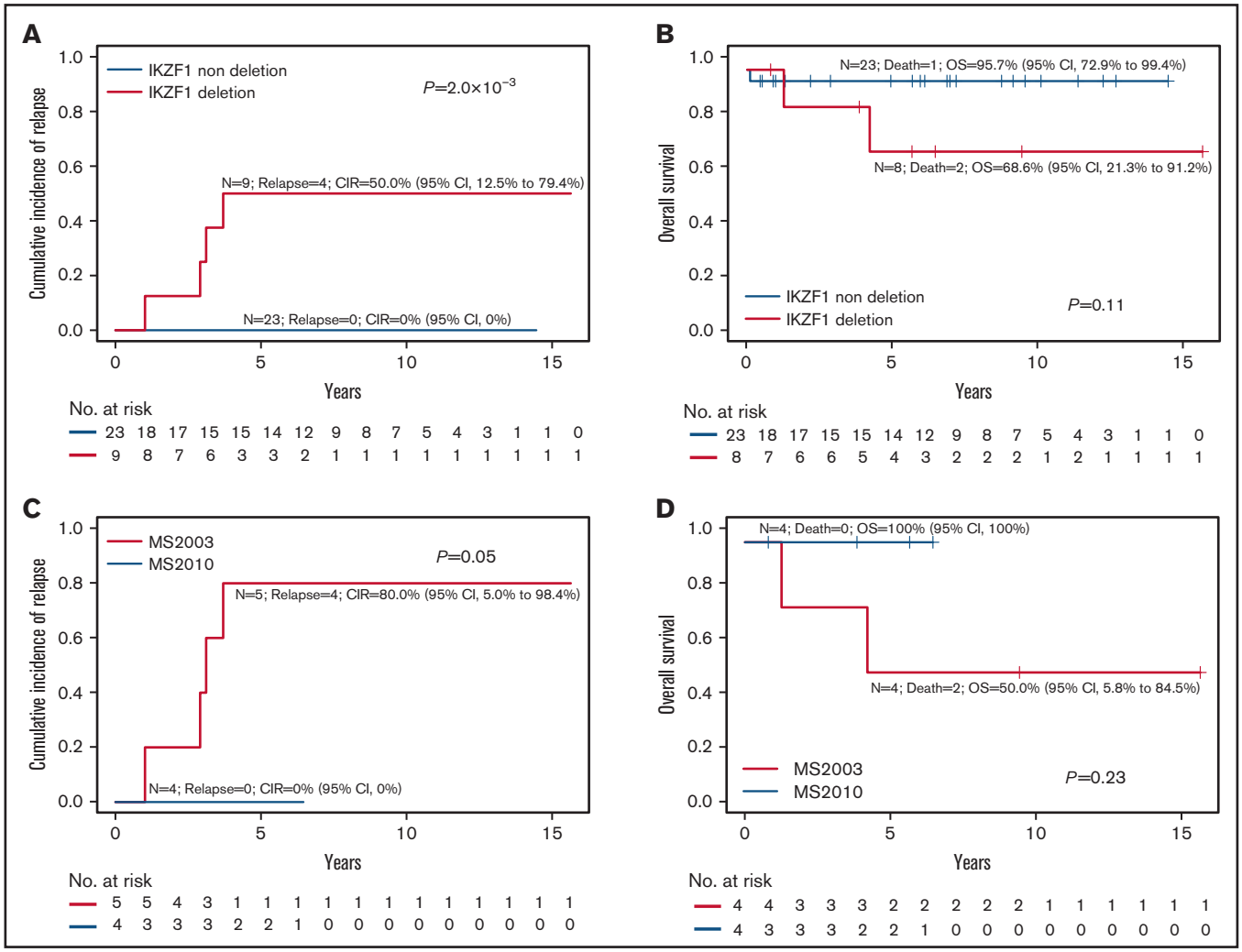

Figure 4. *IKZF1* deletion in *PAX5*alt subtype. Overall outcomes of *PAX5*alt subtype with or without *IKZF1*^{del} based on CIR (A) and OS (B). Outcome of *PAX5*alt subtype with *IKZF1*^{del} analyzed by MS2003 vs MS2010 based on (C) CIR and (D) OS.

suggested that the *DUX4* subtype is indeed favorable, and patients with that subtype do not need intensified HR therapy.

The next question was why none of the patients in Total Therapy Study XVI with *DUX4* were HR. St. Jude researchers used flow-based MRD[44] whereas MS2003 and MS2010 used PCR-based MRD. PCR-based MRD probably overestimated the residual disease because of the monocytic switch in the *DUX4* subtype after treatment.[43] At day 42 of induction, 95% of the patients with *DUX4* in the Total Therapy Study XVI were MRD negative ($\leq 1 \times 10^{-4}$) by flow cytometry compared with only 22% of patients being MRD negative by PCR at EOI in MS2003 and MS2010 (supplemental Table 1). Taken together, the *DUX4* subtype was favorable, and MRD by flow cytometry probably more accurately quantitated the residual disease for patients with *DUX4*.

ERG deletion occurred almost exclusively in *DUX4* B-ALL (92%; n = 23 of 25). Although it represented a secondary event in the *DUX4* subtype, *ERG* deletion was associated with better EOI MRD (Figure 3F), similar to the experience by Zaliova et al.[29] Unsupervised hierarchical clustering showed that *DUX4* subtype with ERG deletion had a distinct signature (Figure 3G). Taken together, our data suggested that *ERG* deletion in *DUX4* subtype was not merely a passenger event that occurs coincidentally; *ERG* deletion in the *DUX4* subtype influenced treatment response. The codeletion of *ERG* with *DUX4* dysregulation is worth exploring in future studies.

The fourth most common subtype of B-ALL, accounting for 10% of our cohort, was *PAX5*alt (Table 1). *PAX5*alt conferred an intermediate risk of relapse with 5-year CIR of 18.1% (95% CI, 6.3%-34.7%). These *PAX5*alt relapses tended to be late (median time to relapse, 2.5 years) and were responsive to initial relapse therapy with 50% long-term survival (including 1 after BM transplantation). Similarly, the Total Therapy Study XVI reported that patients with *PAX5*alt had CIRs of 17.3%, which were late and extramedullary (CIR, 2.5 to 4 years; 50% CNS relapse).[44] Yet patients in the Total Therapy Study XVI with *PAX5*alt who had relapsed were eligible for salvage therapy with an excellent OS of 100% (supplemental Table 5).

The codeletion of *IKZF1* in patients with *PAX5*alt was highly predictive of relapse ($P = 2.0 \times 10^{-3}$; Figure 4A). Because the *PAX5*alt

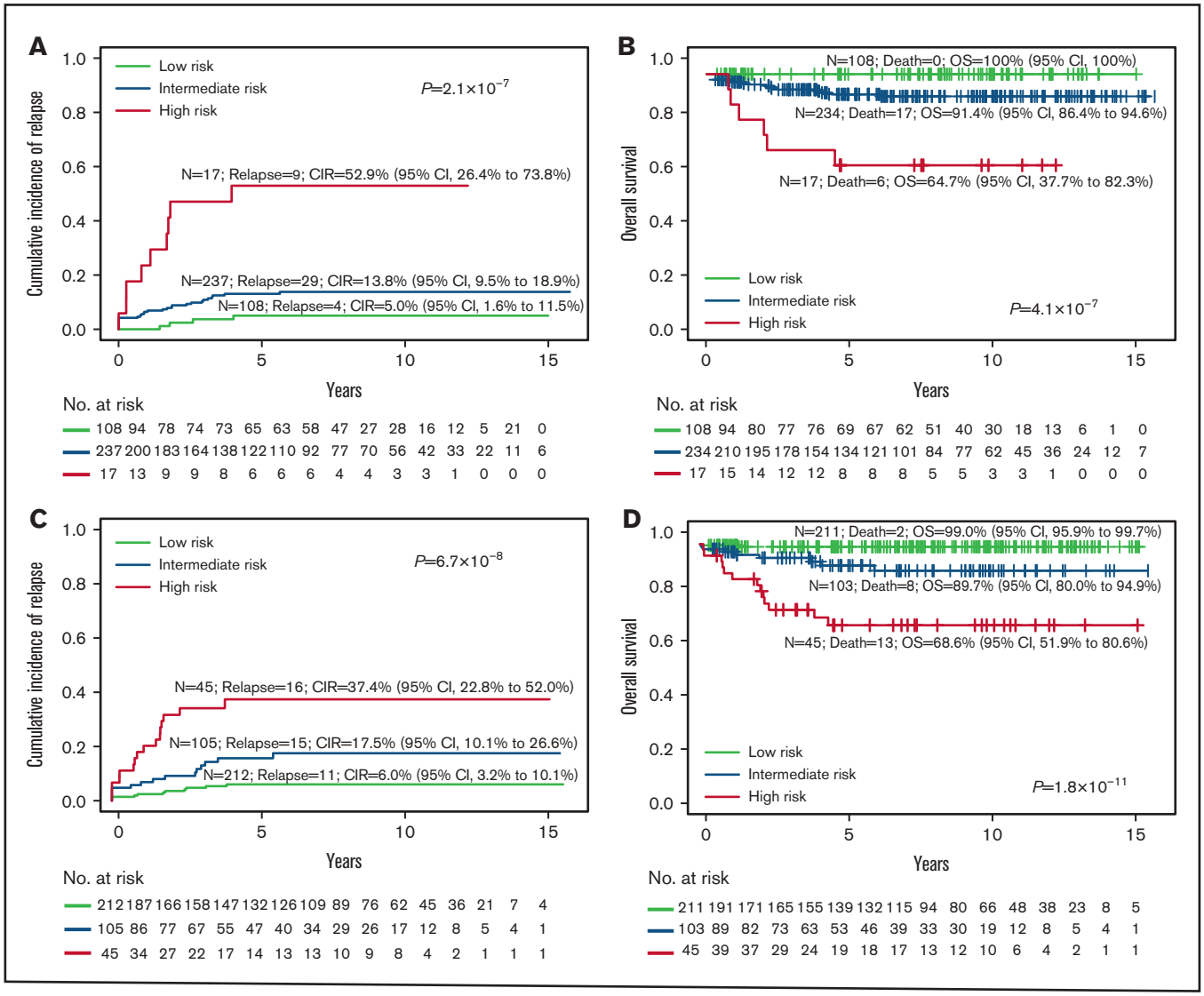

Figure 5. Risk stratification using conventional subtype classification methods compared with RNA-seq. CIR (A) and Kaplan-Meier estimates of OS (B) of risk groups stratified by conventional laboratory tests such as oncogene fusion panels, cytogenetic and DNA index, and risk stratification are limited to *BCR-ABL1*, *KMT2A*, and hypodiploid (including near haploid) as HR, and *ETV6-RUNX1* and hyperdiploid as LR. CIR (C) and Kaplan-Meier estimates of OS (D) of risk groups on the RNA-seq platform with risk stratification of the new groups recently defined. The LR group includes high hyperdiploid, *ETV6-RUNX1*, *DUX4*, and *ZNF384-EP300*; the HR group includes *BCR-ABL1*, *BCR-ABL1*-like, *CRLF2*, hypodiploid, near haploid, *KMT2A*, *MEF2D*, and *TCF3-HLF*.

group was characterized by a high frequency of *PAX5* deletions, all 9 patients who had *PAX5*alt with *IKZF1*^{del} were essentially BFM *IKZF1*^{plus}.[9] Among the subtypes, the *PAX5*alt subtype accounted for most of the *IKZF1*^{plus} subtypes (38%; n = 9 of 24; supplemental Figure 16). Interestingly, in the *PAX5*alt subtype with *IKZF1*^{del}, intensifying treatment in MS2010 trial to the next risk level improved the outcome (CIR, 80% vs 0%; P = .05). In Total Therapy Study XVI, all 4 of the patients with *PAX5*alt who relapsed were those who cleared their MRD at day 42 and did not receive intensified therapy. Unfortunately, we do not know the status of their *IKZF1*^{del}. In the absence of *IKZF1*^{del}, when patients were stratified according to MRD, those with *PAX5*alt had an excellent outcome (n = 23; CIR, 0%). Conversely, the presence of *IKZF1*^{del} in the *PAX5*alt subtype conferred a high risk of relapse (80%; n = 4 of 5) in MS2003, which improved with intensification of therapy (n = 0 of 4; CIR, 0%) in MS2010. This was similar results from the UKALL 2003 trial regarding intrachromosomal amplification of chromosome 21 (iAMP21) in which intensifying therapy abrogated poor prognosis attributed to iAMP21.[45]

We next tested whether our ability to assign 93% of our cohort to 1 of the subtypes with its distinct risk of relapse would help to improve our current PCR MRD-based risk stratification. To avoid overfitting, we based our RNA-seq subtype risk stratification on outcomes published in the literature (supplemental Table 3). We found that RNA-seq subtype stratification was highly predictive of relapse and OS (Figure 5C-D). Specifically, the LR group, which accounted for 59% of the cohort, had excellent outcome (CIR, 6.0%; OS, 99.0%). The HR group (12% of the cohort) accounted for 38% of

Table 2. Multivariable analysis using competing risk regression on CIR and Cox proportional hazards regression on OS

	Competing risk regression on CIR			Cox proportional hazards regression on OS		
Variable	**HR**	**95% CI**	***P***	**HR**	**95% CI**	***P***
RNA-seq risk stratification						
Low*	1.0			1.0		
Intermediate	2.89	1.26-6.61	.01	14.34	1.67-123.53	.02
High	4.85	1.94-12.10	7.2×10^{-4}	31.63	3.71-296.32	1.6×10^{-3}
Age, y						
1-10*	1.0			1.0		
<1	0.72	0.26-2.00	.53	1.06	0.21-5.50	.94
≥10	0.74	0.28-1.97	.54	3.24	1.03-10.17	.04
Sex						
Female*	1.0			1.0		
Male	1.50	0.77-2.95	.23	1.36	0.46-3.98	.58
WBC						
$<50 \times 10^9$/L*	1.0			1.0		
$\geq 50 \times 10^9$/L	1.48	0.77-2.84	.24	1.56	0.59-4.15	.37
Day 33 MRD						
$\leq 1 \times 10^{-4}$*	1.0			1.0		
1×10^{-4} to 1×10^{-2}	2.02	0.91-4.48	.08	2.44	0.71-8.46	.16
$\geq 1 \times 10^{-2}$	8.73	3.57-21.32	2.0×10^{-6}	3.31	0.91-12.07	.07
Protocol						
MS2003*	1.0			1.0		
MS2010	0.46	0.23-0.93	.03	0.38	0.12-1.25	.11

*Reference group.

the relapses and 57% of the deaths. In multivariable analysis, after controlling for age, sex, presenting WBC, EOI MRD, and treatment protocol, RNA-seq risk stratification was independently predictive of relapse and OS (Table 2). In each risk group stratified by RNA-seq, EOI MRD predicted only CIR but not OS (supplemental Figure 15).

There were 3 groups that were assigned on the basis of gene expression similarities with known groups: *ETV6-RUNX1*-like, *ZNF384*-like, and *BCR-ABL1*-like (Table 1). The *ETV6-RUNX1*-like (2% of patients) had an IR profile, which differed from that of *ETV6-RUNX1* (5-year CIR, 12.7% vs 5.2%, $P = .44$; 5-year OS, 88.9% vs 100%, $P = .0044$). *ETV6-RUNX1*-like subtype was associated with a very high frequency of *IKZF1*^{del} (63%), significantly higher than that in *ETV6-RUNX1* (7%; $P = 9.1 \times 10^{-6}$), consistent with previous findings.[3] Most of the patients who had the *ETV6-RUNX1*-like subtype were clustered in a unique sub-branch (Figure 2). These results distinguished *ETV6-RUNX1*-like from the *ETV6-RUNX1* subtype and suggested the risk stratification of the "-like" groups should be considered separately from their established counterparts. This was a retrospective study of subtypes of B-ALL that used RNA-seq. The RNA-seq patients were enriched for EOI MRD positive, and conventionally unclassified patients had the B-Others subtype (supplemental Table 6). Despite these differences, the CIR and OS were not significantly different from those for patients in the main cohort (supplemental Figure 17).

By using the recently published data[44] from Total Therapy Study XVI, we generated an independent test cohort based on our RNA-seq risk groups (supplemental Table 7). We found that our RNA-seq risk groups yielded outcomes similar to those of Total Therapy Study XVI when comparing them to MS2003 and MS2010 (supplemental Table 7). The only exception was that in Total Therapy Study XVI, patients with *BCR-ABL1* received dasatinib and had better outcomes. Taken together, we believe that RNA-seq risk groups could be generalized to real-world applications.

We proposed that RNA-seq be used in a prospective MRD-stratified ALL study to genetically subtype patients with B-ALL. This could substantially improve risk assignment and guide the choice of either adding tyrosine kinase inhibitor or increasing the intensity of therapy. To complement MRD-based risk stratification, we implemented RNA-seq subtype classification and risk stratification workflow for our successor MS2020 trial.[46] The workflow could classify 3 to 10 patients each week by subtype, which would allow timely diagnosis and intervention. RNA-seq could also provide sequence identification of *IGH* disease clones to help design *IGH* PCR MRD markers for MRD quantitation.[47]

In conclusion, RNA-seq can assign up to 93% of patients with B-ALL to a distinct genetic subtype and can help improve risk assignment, even in contemporary MRD-based stratification. The newly identified *DUX4* and *PAX5*alt subtypes, which accounted for the third and fourth most common subtypes of ALL, had distinct clinical characteristics. Despite an excellent outcome, patients with the *DUX4* subtype cleared MRD slowly, and the majority of patients were MRD positive at EOI. The *PAX5*alt subtype with codeletion of *IKZF1* had a high risk of relapse, but this improved with intensified therapy.

Acknowledgments

This work was supported by the Singapore National Medical Research Council Clinician Scientist Awards (NMRC/CSA/0053/2013 and MOH-000277), Children's Cancer Foundation (Singapore), Singapore Tote Board, Goh Foundation (Singapore), and Viva Foundation for Children with Cancer.

The computational work for this article was partially performed using resources at the National Supercomputing Centre in Singapore (https://www.nscc.sg).

Authorship

Contribution: J.J.Y. and A.E.-J.Y. designed the study; T.C.Q., H.P.L., A.M.T., H.A., and A.E.-J.Y. cared for patients and provided study materials and clinical data; Z.L., S.H.R.L., W.H.N.C., Y.L., N.J., E.H.L., E.C.-S., K.H.C., B.L.Z.O., G.S.K., Z.C., S.K.Y.K., J.J.Y., and A.E.-J.Y. collected and assembled the data; K.H.C., Z.C., and S.K.Y.K. provided administrative support; Z.L., S.H.R.L., B.L.Z.O., J.J.Y., and A.E.-J.Y. performed data analysis and designed the figures; and all authors helped write the paper and approved the manuscript.

Conflict-of-interest disclosure: The authors declare no competing financial interests.

ORCID profiles: A.E.-J.Y., 0000-0002-6454-976X; B.L.Z.O., 0000-0001-6184-8935; A.M.T., 0000-0002-9831-3675.

Correspondence: Allen Eng-Juh Yeoh, Viva-University Children's Cancer Centre, KTP-National University Children's Medical Institute, Yong Loo Lin School of Medicine, National University of Singapore, Level 12, National University Health System, Tower Block, 1E Kent Ridge Rd, Singapore 119228; e-mail: paeyej@nus.edu.sg.

RNA-seq data were deposited in European Genome-Phenome Archive with accession numbers EGAS00001001858, EGAS00001003726, and EGAS00001004532.

References

1. Inaba H, Mullighan CG. Pediatric acute lymphoblastic leukemia. *Haematologica.* 2020;105(11):2524-2539.
2. Yeoh EJ, Ross ME, Shurtleff SA, et al. Classification, subtype discovery, and prediction of outcome in pediatric acute lymphoblastic leukemia by gene expression profiling. *Cancer Cell.* 2002;1(2):133-143.
3. Lilljebjörn H, Henningsson R, Hyrenius-Wittsten A, et al. Identification of ETV6-RUNX1-like and DUX4-rearranged subtypes in paediatric B-cell precursor acute lymphoblastic leukaemia. *Nat Commun.* 2016;7(1):11790.
4. Yasuda T, Tsuzuki S, Kawazu M, et al. Recurrent DUX4 fusions in B cell acute lymphoblastic leukemia of adolescents and young adults. *Nat Genet.* 2016;48(5):569-574.
5. Zhang J, McCastlain K, Yoshihara H, et al; St. Jude Children's Research Hospital–Washington University Pediatric Cancer Genome Project. Deregulation of DUX4 and ERG in acute lymphoblastic leukemia. *Nat Genet.* 2016;48(12):1481-1489.
6. Bastian L, Schroeder MP, Eckert C, et al. PAX5 biallelic genomic alterations define a novel subgroup of B-cell precursor acute lymphoblastic leukemia. *Leukemia.* 2019;33(8):1895-1909.
7. Gu Z, Churchman ML, Roberts KG, et al. PAX5-driven subtypes of B-progenitor acute lymphoblastic leukemia. *Nat Genet.* 2019;51(2):296-307.
8. Li JF, Dai YT, Lilljebjörn H, et al. Transcriptional landscape of B cell precursor acute lymphoblastic leukemia based on an international study of 1,223 cases. *Proc Natl Acad Sci U S A.* 2018;115(50):E11711-E11720.
9. Stanulla M, Dagdan E, Zaliova M, et al; International BFM Study Group. IKZF1^{plus} defines a new minimal residual disease-dependent very-poor prognostic profile in pediatric B-cell precursor acute lymphoblastic leukemia. *J Clin Oncol.* 2018;36(12):1240-1249.
10. Yeoh AE, Ariffin H, Chai EL, et al. Minimal residual disease-guided treatment deintensification for children with acute lymphoblastic leukemia: results from the Malaysia-Singapore acute lymphoblastic leukemia 2003 study. *J Clin Oncol.* 2012;30(19):2384-2392.
11. Yeoh AEJ, Lu Y, Chin WHN, et al. Intensifying treatment of childhood B-lymphoblastic leukemia with IKZF1 deletion reduces relapse and improves overall survival: Results of Malaysia-Singapore ALL 2010 Study. *J Clin Oncol.* 2018;36(26):2726-2735.
12. van der Velden VH, Cazzaniga G, Schrauder A, et al; European Study Group on MRD detection in ALL (ESG-MRD-ALL). Analysis of minimal residual disease by Ig/TCR gene rearrangements: guidelines for interpretation of real-time quantitative PCR data. *Leukemia.* 2007;21(4):604-611.
13. Kim D, Pertea G, Trapnell C, Pimentel H, Kelley R, Salzberg SL. TopHat2: accurate alignment of transcriptomes in the presence of insertions, deletions and gene fusions. *Genome Biol.* 2013;14(4):R36.
14. Liao Y, Smyth GK, Shi W. featureCounts: an efficient general purpose program for assigning sequence reads to genomic features. *Bioinformatics.* 2014;30(7):923-930.
15. Love MI, Huber W, Anders S. Moderated estimation of fold change and dispersion for RNA-seq data with DESeq2. *Genome Biol.* 2014;15(12):550.
16. Leek JT, Johnson WE, Parker HS, Jaffe AE, Storey JD. The sva package for removing batch effects and other unwanted variation in high-throughput experiments. *Bioinformatics.* 2012;28(6):882-883.
17. Conover WJ, Iman RL. Rank transformations as a bridge between parametric and nonparametric statistics. *Am Statistician.* 1981;35(3):124-129.
18. Holm S. A simple sequentially rejective multiple test procedure. *Scand J Statist.* 1979;6(2):65-70.

19. Murtagh F, Legendre P. Ward's hierarchical agglomerative clustering method: Which algorithms implement Ward's criterion? *J Classif.* 2014; 31(3):274-295.

20. Nicorici D, Satalan M, Edgren H, et al. FusionCatcher - a tool for finding somatic fusion genes in paired-end RNA-sequencing data. *bioRxiv.* 2014.

21. Van der Auwera GA, Carneiro MO, Hartl C, et al. From FastQ data to high confidence variant calls: the Genome Analysis Toolkit best practices pipeline. *Curr Protoc Bioinformatics.* 2013;43(1110):11.10.1-11.10.33.

22. McLaren W, Gil L, Hunt SE, et al. The Ensembl variant effect predictor. *Genome Biol.* 2016;17(1):122.

23. Dobin A, Davis CA, Schlesinger F, et al. STAR: ultrafast universal RNA-seq aligner. *Bioinformatics.* 2013;29(1):15-21.

24. Gray RJ. A class of K-sample tests for comparing the cumulative incidence of a competing risk. *Ann Statist.* 1988;16(3):1141-1154.

25. Mantel N. Evaluation of survival data and two new rank order statistics arising in its consideration. *Cancer Chemother Rep.* 1966;50(3):163-170.

26. Fine JP, Gray RJ. A proportional hazards model for the subdistribution of a competing risk. *J Am Stat Assoc.* 1999;94(446):496-509.

27. Cox DR. Regression models and life-tables. *J R Stat Soc B.* 1972;34(2):187-220.

28. Nishii R, Baskin-Doerfler R, Yang W, et al. Molecular basis of ETV6-mediated predisposition to childhood acute lymphoblastic leukemia. *Blood.* 2021;137(3):364-373.

29. Zaliova M, Potuckova E, Hovorkova L, et al. *ERG* deletions in childhood acute lymphoblastic leukemia with *DUX4* rearrangements are mostly polyclonal, prognostically relevant and their detection rate strongly depends on screening method sensitivity. *Haematologica.* 2019;104(7):1407-1416.

30. Clappier E, Auclerc MF, Rapion J, et al. An intragenic ERG deletion is a marker of an oncogenic subtype of B-cell precursor acute lymphoblastic leukemia with a favorable outcome despite frequent IKZF1 deletions. *Leukemia.* 2014;28(1):70-77.

31. Harvey RC, Mullighan CG, Wang X, et al. Identification of novel cluster groups in pediatric high-risk B-precursor acute lymphoblastic leukemia with gene expression profiling: correlation with genome-wide DNA copy number alterations, clinical characteristics, and outcome. *Blood.* 2010;116(23): 4874-4884.

32. Den Boer ML, van Slegtenhorst M, De Menezes RX, et al. A subtype of childhood acute lymphoblastic leukaemia with poor treatment outcome: a genome-wide classification study. *Lancet Oncol.* 2009;10(2):125-134.

33. Cario G, Zimmermann M, Romey R, et al. Presence of the P2RY8-CRLF2 rearrangement is associated with a poor prognosis in non-high-risk precursor B-cell acute lymphoblastic leukemia in children treated according to the ALL-BFM 2000 protocol. *Blood.* 2010;115(26):5393-5397.

34. Palmi C, Vendramini E, Silvestri D, et al. Poor prognosis for P2RY8-CRLF2 fusion but not for CRLF2 over-expression in children with intermediate risk B-cell precursor acute lymphoblastic leukemia. *Leukemia.* 2012;26(10):2245-2253.

35. Gu Z, Churchman M, Roberts K, et al. Genomic analyses identify recurrent MEF2D fusions in acute lymphoblastic leukaemia. *Nat Commun.* 2016; 7:13331.

36. Liu YF, Wang BY, Zhang WN, et al. Genomic profiling of adult and pediatric B-cell acute lymphoblastic leukemia. *EBioMedicine.* 2016;8:173-183.

37. Suzuki K, Okuno Y, Kawashima N, et al. MEF2D-BCL9 fusion gene is associated with high-risk acute B-cell precursor lymphoblastic leukemia in adolescents. *J Clin Oncol.* 2016;34(28):3451-3459.

38. Ohki K, Kiyokawa N, Saito Y, et al; Tokyo Children's Cancer Study Group (TCCSG). Clinical and molecular characteristics of *MEF2D* fusion-positive B-cell precursor acute lymphoblastic leukemia in childhood, including a novel translocation resulting in *MEF2D-HNRNPH1* gene fusion. *Haematologica.* 2019;104(1):128-137.

39. Minson KA, Prasad P, Vear S, et al. t(17;19) in children with acute lymphocytic leukemia: A report of 3 cases and a review of the literature. *Case Rep Hematol.* 2013;2013:563291.

40. Fischer U, Forster M, Rinaldi A, et al. Genomics and drug profiling of fatal TCF3-HLF-positive acute lymphoblastic leukemia identifies recurrent mutation patterns and therapeutic options. *Nat Genet.* 2015;47(9):1020-1029.

41. Inukai T, Hirose K, Inaba T, et al. Hypercalcemia in childhood acute lymphoblastic leukemia: frequent implication of parathyroid hormone-related peptide and E2A-HLF from translocation 17;19. *Leukemia.* 2007;21(2):288-296.

42. Hirabayashi S, Butler ER, Ohki K, et al. Clinical characteristics and outcomes of B-ALL with ZNF384 rearrangements: a retrospective analysis by the Ponte di Legno Childhood ALL Working Group [published online ahead of print on 10 March 2021]. *Leukemia.*

43. Novakova M, Zaliova M, Fiser K, et al. DUX4r, ZNF384r and PAX5-P80R mutated B-cell precursor acute lymphoblastic leukemia frequently undergo monocytic switch. *Haematologica.* 2021;106(8):2066-2075.

44. Jeha S, Choi J, Roberts KG, et al. Clinical significance of novel subtypes of acute lymphoblastic leukemia in the context of minimal residual disease-directed therapy. *Blood Cancer Discov.* 2021;2(4):326-337.

45. Moorman AV, Robinson H, Schwab C, et al. Risk-directed treatment intensification significantly reduces the risk of relapse among children and adolescents with acute lymphoblastic leukemia and intrachromosomal amplification of chromosome 21: a comparison of the MRC ALL97/99 and UKALL2003 trials. *J Clin Oncol.* 2013;31(27):3389-3396.

46. Li Z, Jiang N, Lim EH, Chin WHN, Yeoh AE-J. Role of transcriptome sequencing in clinical diagnosis of B-cell acute lymphoblastic leukemia. *Leukemia.* 2021;35(7):2135-2137.

47. Li Z, Jiang N, Lim EH, et al. Identifying IGH disease clones for MRD monitoring in childhood B-cell acute lymphoblastic leukemia using RNA-Seq. *Leukemia.* 2020;34(9):2418-2429.